

Effects of low and high molecular mass PEG incorporation into different types of poly(ether-*b*-amide) copolymers on the permeation properties of CO₂ and CH₄

Navid Azizi¹ · Hamid Reza Mahdavi¹ · Mojgan Isanejad¹ · Toraj Mohammadi¹ 

Received: 8 May 2017 / Accepted: 31 July 2017 / Published online: 16 August 2017
© Springer Science+Business Media B.V. 2017

Abstract Blend membranes were prepared by incorporating two types of polyethylene glycol (PEG) (molecular masses of 400 and 1000 g mol⁻¹) into three grades of poly(ether-*block*-amide) (PEBAX), namely PEBAX 1074, PEBAX 1657, and PEBAX 2533. The PEGs, which were used as blending agents, were employed at mass fractions ranging from 10 to 40 wt.% based on the mass of PEBAX. The gas separation performance of each neat or blend membrane, comprising its CO₂ and CH₄ permeabilities and its ideal CO₂/CH₄ selectivity, was studied at room temperature (25 °C) and at pressures of 2–8 bar. X-ray diffraction (XRD) and attenuated total reflection Fourier transform infrared spectroscopy (ATR-FTIR) analyses were used to determine the crystallinities of and the chemical bonds in the prepared membranes, respectively. Scanning electron microscopy (SEM) was also utilized to observe the morphologies of the membranes. The results obtained from experimental investigations showed that the incorporation of low molecular mass PEG significantly increased the permeability but only slightly affected the ideal CO₂/CH₄

selectivity, while the incorporation of high molecular mass PEG decreased the permeability considerably but sharply increased the ideal CO₂/CH₄ selectivity. This behavior intensified as the polyether content of the PEBAX was decreased.

Keywords Low molecular mass PEG · High molecular mass PEG · PEBAX · Blend membrane · Gas separation

Introduction

In the past few decades, one of the main problems encountered by the gas industry has been the presence of CO₂ in natural gas, as it reduces the heating value of the gas and wastes pipeline capacity. Many technologies are available for the removal of CO₂ from gas streams, such as physical absorption, adsorption, and cryogenic processes. However, each of these technologies has its particular advantages and disadvantages [1–3]. Membrane-based gas separation technology has recently become of interest to the gas industry because of its inherent advantages, such as its smaller footprint and lower capital and operating costs in comparison with other, more traditional, separation technologies [4–6]. Polymers are usually utilized to fabricate membranes because of their low cost and high processability. However, the inverse relationship between the permeability and selectivity of polymeric membranes limits their widespread utilization in the gas industry; therefore, several studies have attempted to overcome this trade-off by modifying polymeric membranes to improve their separation performance [7–10].

Ethylene oxide (EO) units have been identified as favorable chemical groups to incorporate into polymeric membranes used for selective CO₂ separation, as the ether oxygen interacts with CO₂, resulting in high CO₂ solubility selectivity. It was recently shown that copolymer networks containing

Research highlights • PEBAX /PEG blend membranes were developed.
• The incorporation of two types of PEGs into three grades of PEBAX polymers was investigated.
• An experimental study of the separation of CO₂/CH₄ using blend membranes was proposed.
• The effects of PEG molecular mass, PEG content, PE content of the polymer matrix, and feed pressure on the CO₂/CH₄ separation achieved with each membrane were discussed.
• The effects of PEG incorporation on membrane morphology were studied.

✉ Toraj Mohammadi
torajmohammadi@iust.ac.ir

¹ Research and Technology Centre of Membrane Processes, Faculty of Chemical Engineering, Iran University of Science and Technology (IUST), Narmak, Tehran, Iran

short and noncrystallizable EO segments exhibit outstanding CO₂/CH₄ separation performance. Yave et al. showed that the addition of 50 wt.% PEG-dimethylether (PEG-DME) to PEBAX 1657 increases the permeability of CO₂ from 78 to 606 barrer and the CO₂/H₂ selectivity from 9.1 to 14.9 at 30 °C and 300 mbar due to the increased CO₂ diffusion and solubility in the blend membranes [11].

In the work reported in the present paper, three grades of polyether-*block*-amide (PEBAX 1657, PEBAX 2533, and PEBAX 1074) were employed as the base polymeric materials for the synthesis of blend membranes. PEBAX is a thermoplastic polymer with two separated microphases: a polyamide (PA) hard phase and a polyether (PE) soft phase. In these polymers, crystalline PA domains providing mechanical strength are located between PE domains, preventing their crystallization and therefore greatly enhancing chain mobility [12]. The favorable interactions of the polar ether oxygens with CO₂ result in high solubility selectivity for CO₂ over nonpolar gases such as CH₄ [13–15]. The main differences between these three grades of PEBAX are their different PA and PE contents. Table 1 shows the compositions and physical properties of these three different types of PEBAX.

The separation performance of polymeric membranes can be improved using two general techniques: synthesizing new polymers and modifying existing commercial polymers with different additives. These additives can be organic materials such as polymers or inorganic compounds such as metal oxide nanoparticles [16, 17]. The separation efficiency of polymeric blend membranes is influenced by the features of the base polymer and the incorporated additives; therefore, careful selection of the additives to get an efficient membrane with high separation performance is necessary. The addition of various plasticizers such as PEGs with different molecular masses to the base polymer can have different effects on the gas transport properties of the resulting blend membranes. PEG can dissolve considerable amounts of sour gas due to its chain flexibility [18]. The plasticizers can operate as spacers, separating macromolecular chains (i.e., increasing the free volume) and thus decreasing intermolecular attractive forces, increasing chain mobility, and consequently facilitating the diffusion of adsorbed molecules by lowering the activation energy. Moreover, inserting plasticizers between the polymer

chains reduces the glass transition temperature of the polymer due to local segmental motions. As can be seen in the literature, there have been many studies of the influences of various plasticizers on the morphologies and gas transport properties of polymer blends [7, 19–21]. In this study, to examine the influences of different fillers on the gas permeabilities of blend membranes, two types of PEG (PEG 400 and PEG 1000) were blended with different grades of PEBAX. The physical properties of these two PEGs with different molecular masses are presented in Table 2.

Many researchers have synthesized PEBAX/PEG blend membranes for gas separation applications. Recently, Zhao et al. [22] prepared PEBAX 1657-PEG 200/zeolite Y composite membranes for CO₂ capture from flue gas. They blended different amounts of PEG 200 with PEBAX (25, 50, and 75 wt.% based on the mass of PEBAX) via solution blending. Gas permeation experiments showed that increasing the PEG content from 0 to 75 wt.% caused the CO₂ permeance to enhance from 102 to 745 GPU. The permeation results also revealed that the CO₂/N₂ selectivity values of the prepared membranes did not change much after PEG was incorporated into the PEBAX matrix. Mahmoudi et al. [23] prepared PEBAX 1657/PEG/NaX nanocomposite membranes for CO₂/CH₄ separation. In their study, PEG200 was used as a blending agent at different loadings (10%, 20%, and 30%). The results of their investigation demonstrated that the separation efficiency of the membrane with 30 wt.% PEG and 10 wt.% nanozeolite was the highest among all of the prepared membranes. The CO₂ permeability and ideal CO₂/CH₄ selectivity for the membrane were 95 barrer and 45, respectively. Ghadimi et al. [24] prepared PEBAX 1657/PEGDA blend membranes for the separation of CO₂ from H₂. They used different amounts (20, 40, and 60 wt.%) of poly(ethylene glycol diacrylate) with a molecular mass of 600 (PEGDA-600) to prepare the blend membranes. The results obtained from permeation experiments in their investigation indicated that increasing the PEG loading enhanced the permeability of CO₂ whereas that of H₂ did not alter significantly. The results also indicated that at 25 °C, the PEBAX/PEGDA blend membrane with 20 wt.% of PEGDA exhibited the best CO₂/H₂ separation performance of all the membranes. The corresponding CO₂ permeability and ideal CO₂/H₂ selectivity values were 140

Table 1 Physical properties of the different grades of PEBAX

Property	PEBAX 1074	PEBAX 1657	PEBAX 2533
Polyether content (wt.%)	55	60	80
Density (g cm ⁻³)	1.07	1.14	1
Water absorption at 23 °C and 24 h in water (wt.%)	48	120	1.2
Melting point (°C)	158	204	134
Glass transition temperature (°C)	-55	-56	-65
Stress at break (MPa)	30	32	32

Table 2 Physical properties of different grades of PEG

	PEG 400	PEG 1000
Chemical formula	$\text{H}(\text{CH}_2\text{CH}_2\text{O})_n\text{OH}$	
Molecular mass (g mol^{-1})	380–420	950–1050
Density (g cm^{-3})	1.13	1.2
Melting point ($^{\circ}\text{C}$)	4–8	33–40

barrer and 16, respectively. In research carried out by Car et al. [12], PEBAX 1657 blend membranes were prepared by adding 0–50% of PEG 200 to investigate the effect of the low molecular weight PEG on the gas separation performance of the membranes for H_2 , N_2 , CH_4 , and CO_2 . It was observed that, due to the decrease in the total crystallinity of the membranes and the increased interactions between the CO_2 molecules and EO groups when the membrane contained 50 wt.% rather than 0 wt.% PEG 200, the CO_2 permeability increased twofold (from 73 to 151 barrer at 30°C) while the CO_2/CH_4 selectivity remained almost constant. In another work, Reijerkerk et al. [13] studied the permeability of CO_2 through dense blend membranes fabricated from PEBAX 1657 and a PEG 200-based additive. To obtain a PEG with both high CO_2 selectivity and high CO_2 permeability, they combined PEG with PDMS. The gas permeation results at 4 bar and 35°C showed that the addition of 50 wt.% PEG-PDMS to the base polymer, PEBAX 1657, increased CO_2 permeability from 100 to 530 barrer due to diffusive permeation, while the CO_2/CH_4 selectivity slightly decreased from 16.1 to 10.8. The incorporation of PEG 200 into PEBAX 1657 in membranes also resulted in an increase in CO_2 permeability from 98 to 172 and a decrease in the ideal CO_2/CH_4 selectivity from 16.1 to 15.7 as the content of PEG 200 was increased from 0 to 50 wt.%.

A recent study by Wang et al. [14] investigated three-component hybrid membranes (PEBAX-PEG-MWCNT) for CO_2/N_2 and CO_2/CH_4 separations. The results indicated that the MWCNT dispersion was improved upon the hydrophilic modification of nanotubes with PEG, but their incorporation decreased the ideal CO_2/CH_4 selectivity as the chain mobility was enhanced. The CO_2 permeability of the membrane increased as the amorphous phase was enhanced by increasing the PEG content from 0 to 40 wt.%. PEG-functionalized POSS was used by Rahman et al. [15] to evaluate the effect of incorporating this additive into the base polymers PEBAX 1657 and 2533. At 30°C , the incorporation of 30 wt.% PEG-POSS increased CO_2 permeability twofold for both the PEBAX 1657 and the PEBAX 2533 membranes (from 75 to 150 and 100 barrer, respectively). The selectivity of the resulting membrane was barely affected by the addition of PEG-POSS to PEBAX 1657, but it was affected when PEG-POSS was added to PEBAX 2533. It was concluded that PEG-POSS acts as a nanofiller and plays an important role in improving the viability of PEG-containing PEBAX

membranes. Khosravi et al. [16] combined the highly permeable poly(propylene glycol) (PPG) with the highly selective PEG to prepare blend membranes from the block copolymer PEBAX 1657. They studied the effect of the level of PEG loading (10–50 wt.%), the feed pressure (3–10 bar), and the operating temperature (-10 to 30°C) on the CO_2/CH_4 separation performance of the membrane. The results showed that when PPG was randomly distributed in PEG, the CO_2 permeability increased from 84 to 677 barrer, while the CO_2/CH_4 selectivity did not change significantly.

In the present study, the blend membranes were fabricated by incorporating two types of poly(ethylene glycol) (PEG 400 and PEG 1000) into three grades of poly(ether-block-amide): PEBAX 1657, PEBAX 2533, and PEBAX 1074. Scanning electron microscopy (SEM), Fourier transform infrared (FT-IR) spectroscopy, and X-ray diffraction (XRD) analysis were utilized to characterize the fabricated membranes. CO_2 and CH_4 permeation experiments through all the membranes were also carried out to evaluate the separation performance of the prepared membranes.

Experiments

Materials

PEBAX 1074, PEBAX 1657, and PEBAX 2533 elliptic pellets were supplied by Arkema Inc. (King of Prussia, PA, USA). PEG 400 and PEG 1000 were obtained from Merck (Darmstadt, Germany). DMF, which was used as solvent, was also purchased from Merck. The CO_2 and CH_4 gases used in permeation experiments had purities of 99.995% and were acquired from Farafan Gas Tehran Company (Tehran, Iran). All materials and gases were used as received, except for the PEBAX pellets.

Membrane preparation

The PEBAX pellets were placed in a vacuum oven at 80°C for 6 h for degassing and moisture removal. In the current investigation, the neat PEBAX 1074, PEBAX 1657, and PEBAX 2533 membranes were fabricated via a solution casting method. The 4.5 wt.% polymeric solutions were prepared by dissolving PEBAX pellets in DMF under stirring for 3 h at a specified temperature. The dissolution temperatures were 115, 105, and 80°C for PEBAX 1074, PEBAX 1657, and PEBAX 2533, respectively. A steel filter was applied to the prepared polymer solutions to obtain clear and homogeneous solutions. Thereafter, the solutions were cast on glass Petri dishes and dried at 50°C for 24 h. The resulting membrane films were finally peeled off the Petri dishes.

To fabricate the blend membranes, PEG was added to DMF at levels of 10, 20, 30, and 40 wt.% (based on the mass of the

polymer) and stirred magnetically for 30 min. Thereafter PEBAX pellets were gradually added to the solution in specific amounts, and the solution was stirred again for 3 h at the specified temperatures mentioned before. The prepared solution was cast on glass Petri dishes after filtration and dried in the same manner as the neat membranes. After complete evaporation of the solvent, the prepared membranes were cooled at ambient temperature and stored in a desiccator before further characterization. The resulting dense flat-sheet membranes had thicknesses of between 50 and 70 μm .

Membrane characterization

X-ray diffraction (XRD)

X-ray diffraction (XRD) analysis was used to investigate the crystalline morphologies of the polymeric membranes, especially the dense ones, in order to determine their permeabilities and selectivities [25]. XRD measurements were performed using a JDX-8030 diffractometer (JEOL, Tokyo, Japan). X-rays of wavelength 1.5406 \AA were generated by a Cu K α source. The diffraction angle (2θ) was varied from 5° to 70° at a scan rate of $0.01^\circ \text{ s}^{-1}$ to identify the crystal structure.

Attenuated total reflection Fourier transform infrared spectroscopy (ATR-FTIR)

Attenuated total reflection Fourier transform infrared spectroscopy (ATR-FTIR) can determine the structural characteristics of and specific functional groups in polymeric membranes as a means to predict their performance [26]. Therefore, Fourier transform infrared spectroscopy (FTIR) was carried out via a Shimadzu (Kyoto, Japan) 8400S spectrometer with an attenuated total reflectance (ATR) accessory. All spectra were collected from 4000 to 400 cm^{-1} at room temperature on wafers including 100 mg of dry KBr and about 1 mg of the sample, with a spectral resolution of 2 cm^{-1} .

Scanning electron microscopy (SEM)

Since the gas permeation properties of a membrane are mainly influenced by its morphology, scanning electron microscopy (SEM) was applied to investigate the effects of morphology on membrane performance [27]. All samples were cryogenically fractured in liquid nitrogen and coated with gold under vacuum before scanning. Cross-sectional images of membranes were obtained using a VEGA\ (TESCAN, Brno-Kohoutovice, Czech Republic) microscope.

Gas permeation module and setup

In order to measure gas permeation through the prepared membranes, an experimental setup was used that allowed

gas permeation measurements to be taken at constant volume or constant pressure. For this purpose, the membranes were placed in a membrane module consisting of two detachable parts (manufactured from stainless steel, grade 316) in a cross-flow mode. Two rubber O-rings were also used to provide a pressure-tight seal between the membrane and the module. The effective diameter of the membrane was about 5.2 cm. Some pressure regulators were utilized to adjust the pressure used in the experiments. A schematic view of the membrane module and the experimental setup is presented in Fig. 1.

Gas permeation experiments

A constant-pressure method was used in the experiments to determine pure CO_2 and CH_4 gas permeation through the prepared membranes. A bubble flow meter was utilized to determine the volumetric flow rate of the permeate gas. Also, different pressures of 2, 4, 6, and 8 bar were employed at temperature of 25°C . When the steady state condition was reached (after 2 h), both gas permeabilities were calculated as follows [28]:

$$P_i = \frac{Q_i \times l}{\Delta p \times A}. \quad (1)$$

In this equation, P_i is the permeability coefficient of gas i (in barrer, where 1 barrer = $10^{-10} \text{ cm}^3 \text{ (STP) cm}^{-1} \text{ s}^{-1} \text{ cmHg}^{-1}$), Q_i is the volumetric flow rate of gas i ($\text{cm}^3 \text{ (STP) s}^{-1}$), l is the membrane thickness (cm), Δp is the transmembrane pressure difference (cmHg), and A is the effective membrane area (cm^2). Furthermore, the ideal selectivity of a membrane for gases i and j (α_{ij}) was determined using pure gas permeation data as follows [29]:

$$\alpha_{ij} = \frac{P_i}{P_j}. \quad (2)$$

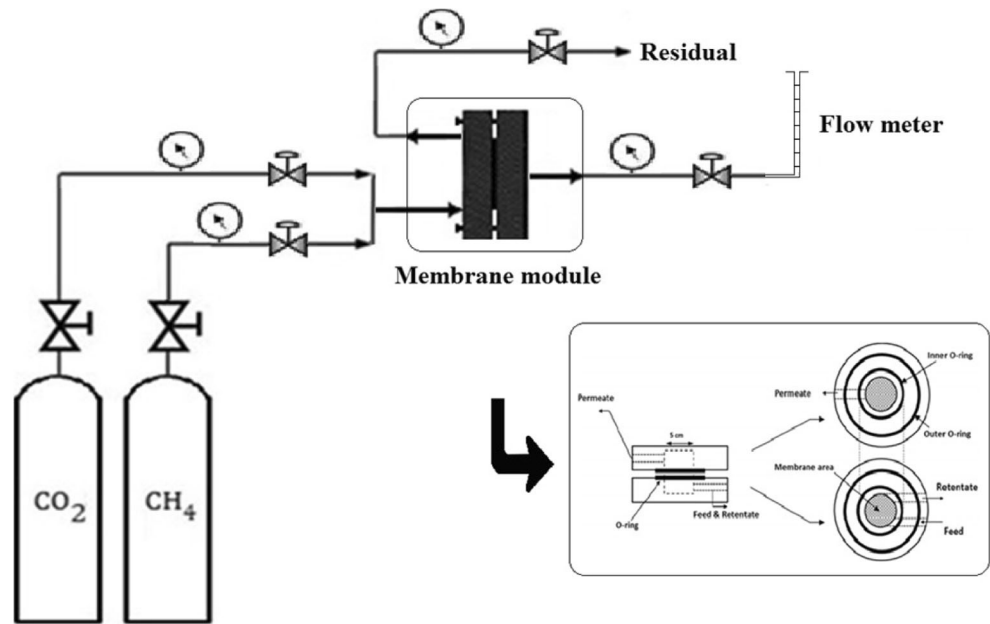
Results and discussion

Membrane characterization

XRD

XRD patterns for the fabricated membranes are shown in Fig. 2. PEBAX is a semicrystalline polymer. The PA crystalline segments in the prepared membranes present strong diffraction peaks, while the PE segments show weak diffraction peaks. Additionally, the amorphous and crystalline areas mainly determine the intensities and locations of diffraction peaks in the patterns [30]. The membrane crystallinity is proportional to the crystalline diffractogram area, particularly the crystalline peak intensity. Furthermore, the

Fig. 1 Schematic view of the module and setup used to perform the gas permeation experiments



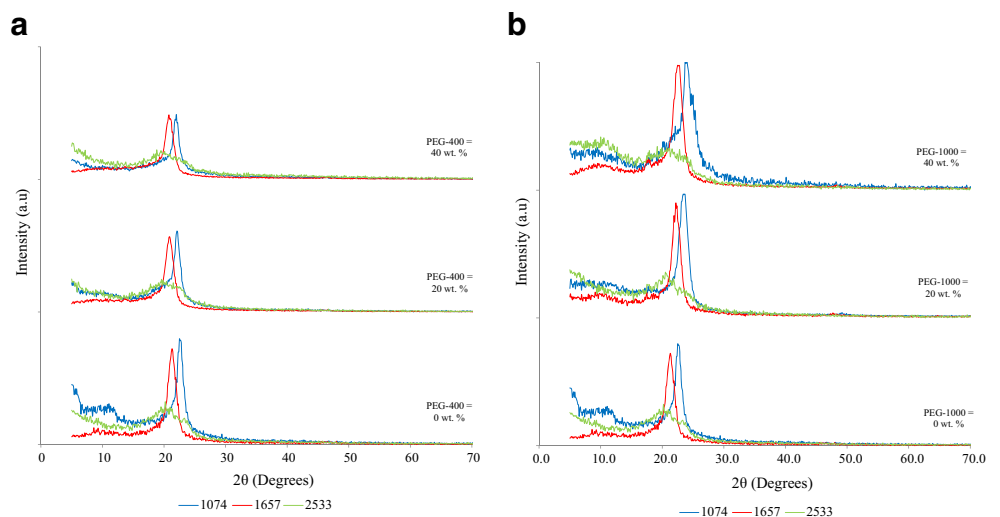
d spacing is a measure of the distance between polymer chains, which is inversely proportional to the crystalline peak positions (2θ values), based on Bragg's equation $n\lambda = 2d\sin\theta$ [7, 31, 32].

As seen in the figure, the prepared neat PEBAX 1074, PEBAX 1657, and PEBAX 2533 membranes present strong diffraction peaks that can be attributed to their PA segments at 22.5° , 21.8° , and 20.2° , respectively. The PE regions of the neat PEBAX 1074 and PEBAX 1657 membranes provide weak diffraction peaks at 10.9° and 9.8° , respectively, while the neat PEBAX 2533 membrane does not present any diffraction peak arising from its PE regions [7, 31, 33]. As can be observed, upon increasing the PE content, the crystalline peak intensities of the neat membranes decrease because their crystallinities reduce. In fact, the neat PEBAX 2533

membrane has the lowest crystallinity due to its high PE content, while the neat PEBAX 1074 membrane has the highest crystallinity because of its high PA content. Based on the crystalline peak positions, it can be concluded that the *d* spacing varies with the membrane as follows: PEBAX 2533 > PEBAX 1657 > PEBAX 1074.

The addition of PEG 400 as a low molecular mass additive leads to lower crystalline peak intensities and lower 2θ values. Thus, the membrane crystallinity is reduced and the *d* spacing is increased. These are due to the increased chain mobility of PEG 400, reduced interchain hydrogen bonding, and therefore a reduction in the cohesive energy between the crystalline segments. Comparison of the XRD patterns for the three types of blend membranes indicated that the order of crystallinity and *d* spacing are similar to those of the neat membranes.

Fig. 2a–b Effects of a PEG 400 and b PEG 1000 on the XRD spectra of the prepared membranes



Moreover, the incorporation of PEG 400 affects PEBAX 1074 more severely than the two other grades. In other words, the intensities and positions of the crystalline peaks for PEBAX 1074 change more because it contains more PA blocks that are connected by interchain hydrogen bonding, and so the addition of PEG 400 disturbs more of this bonding than when the other grades of PEBAX are used. Also, increasing the content of PEG 400 in the polymer matrix leads to greater changes in the crystallinity of the polymeric blend membrane [7, 24].

The addition of PEG 1000 as a high molecular mass additive leads to higher crystalline peak intensities and higher values of 2θ . Thus, the crystallinity goes up and the d spacing decreases. These are due to the lower chain mobility of PEG 1000, increased interchain hydrogen bonding, and thus an increase in the cohesive energy between the crystalline segments. Comparison of the XRD patterns of the three types of blend membranes indicated that the order of crystallinity and d spacing are similar to those seen for the neat membranes. Moreover, the addition of PEG 1000 affects PEBAX 2533 more than it does the two other polymers. In other words, the intensities and positions of the crystalline peaks in PEBAX 2533 change more, which is because it contains more PE blocks. These PE blocks are not connected by interchain hydrogen bonds and the addition of PEG 1000 facilitates the formation of such bonds. Also, increasing the content of PEG 1000 in the polymer matrix leads to greater changes in the crystallinity of the polymeric blend membrane [7].

ATR-FTIR

The effects of adding PEG to different grades of PEBAX were also investigated using ATR-FTIR spectra, as presented in Fig. 3. As shown, the peak observed at around 1112 cm^{-1}

for the neat PEBAX 1074, PEBAX 1657, and PEBAX 2533 membranes was assigned to stretching vibrations of C–O–C (ether group) in the soft segments. The peak at 1626 cm^{-1} was attributed to stretching vibrations of C=O (carbonyl) in H–N–C=O and that at 1734 cm^{-1} was assigned to O–C=O (another carbonyl), both in the hard segments. The peak at 1548 cm^{-1} was assigned to bending vibrations of N–H in the PA segments, and the peaks at 3272 and 3292 cm^{-1} were assigned to N–H stretching vibrations. The peaks at 2846 – 2962 and 1460 cm^{-1} were assigned to bending and stretching vibrations of aliphatic C–H, respectively. It should be mentioned that the peak at 3450 – 3650 cm^{-1} is related to O–H groups resulting from C=O···H–N interchain hydrogen bonding [7, 24, 26, 29, 34–37].

The functional groups of PEG 400 and PEG 1000 were also investigated based on their ATR-FTIR spectra, as shown in Figs. 3a and b, respectively. Peaks located at 700 – 1000 and 1000 – 1300 cm^{-1} were assigned to C–H out-of-plane and in-plane bending vibrations, respectively. Moreover, peaks at 1250 cm^{-1} and 1104 cm^{-1} were assigned to C–C and C–O, respectively. Observed peaks at 2853 and 2926 cm^{-1} were attributed to symmetric and asymmetric stretching vibrations. A peak at 1352 cm^{-1} was assigned to bending vibrations of C–H. Peaks at 2875 and 2966 cm^{-1} correspond to symmetric and asymmetric stretching vibrations, respectively, and the peak at 1460 cm^{-1} is due to bonding vibrations of the CH₂ group. The broad peak at 3050 – 3700 cm^{-1} was assigned to the O–H group [38].

The effects of incorporating PEG 400 and PEG 1000 into the PEBAXs were further investigated via ATR-FTIR, as illustrated in Fig. 3. Comparison of the ATR-FTIR spectra of the blend membranes with those of the neat membranes showed that most of the peaks characteristic of the functional groups in the neat PEBAX are also observed in the blend membrane spectra [7].

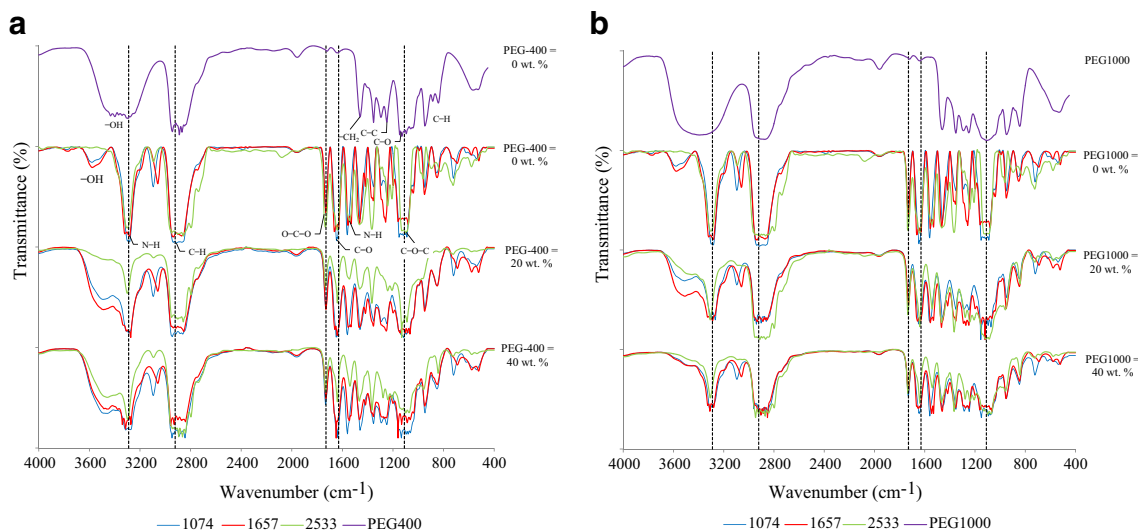


Fig. 3a–b Effects of PEG 400 and PEG 1000 on the ATR-FTIR spectra of the prepared membranes

SEM

SEM images of the membranes prepared with different grades of PEBAX and different types and amounts of PEG are presented in Fig. 4. According to Fig. 4a–c, the cross-sectional morphologies of the neat membranes (for PEBAX 1074, 1657, and 2533) are uniform and show dense structure with a lack of any notable defects [24, 26]. Addition of PEG 400 to the PEBAX matrices decreased the crystallinity of the blend

membranes due to the elimination of intermolecular hydrogen bonds and increasing PE content. The mentioned crystals can be considered physical crosslinks that can regularize the polymeric matrix of the membrane. This can create an irregular and convoluted structure in the blend membranes, as illustrated by Fig. 4d–i [20, 24, 26]. On the other hand, the incorporation of PEG 1000 into the PEBAX matrices increases their crystallinity but decreases their structural uniformity due to immiscibility and phase separation. In other words,

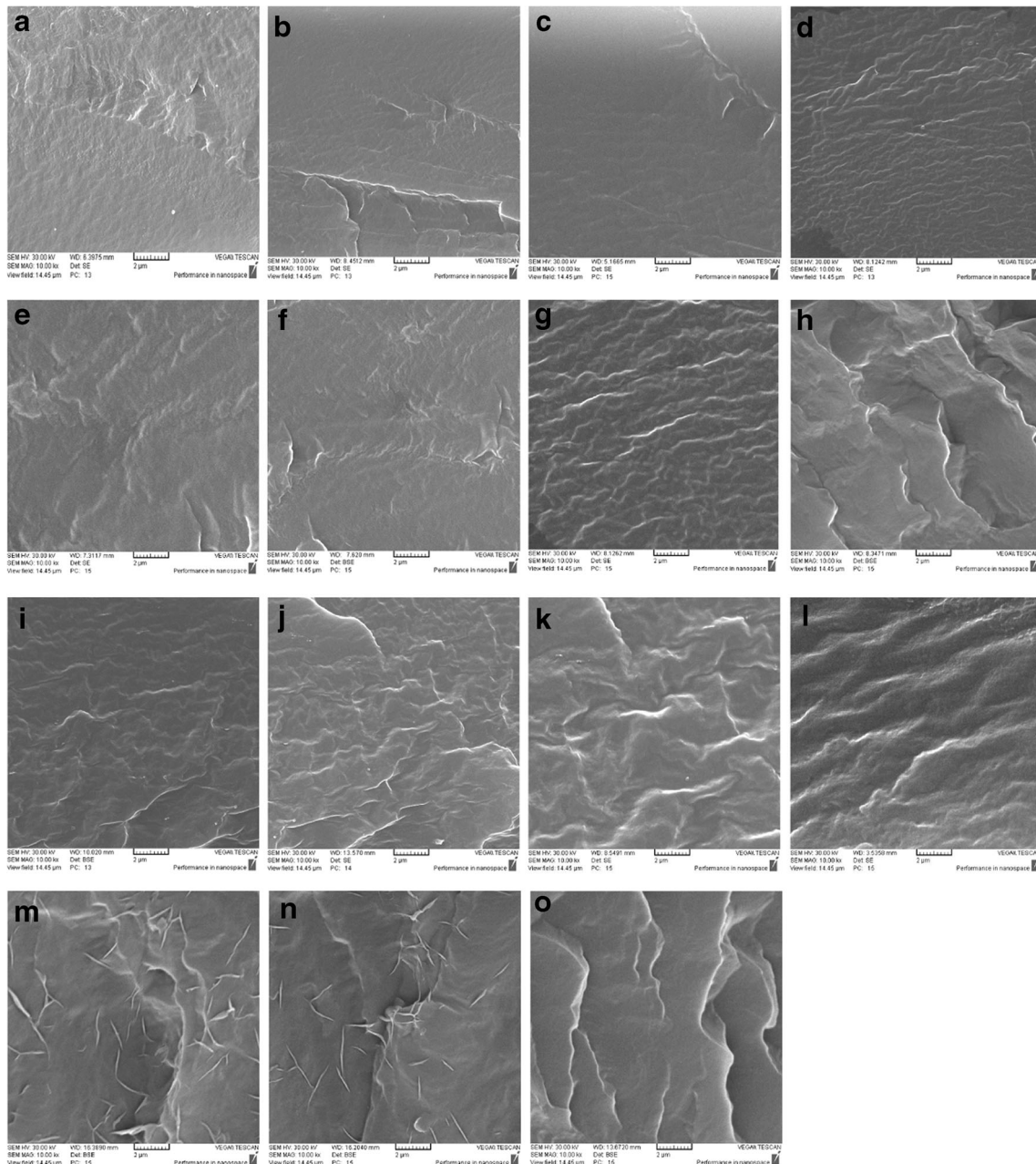


Fig. 4a–o Cross-sectional SEM images of the prepared membranes. **a** Neat PEBAX 1074, **b** neat PEBAX 1657, **c** neat PEBAX 2533, **d** PEBAX 1074/PEG 400 (20 wt.%), **e** PEBAX 1657/PEG 400 (20 wt.%), **f** PEBAX 2533/PEG 400 (20 wt.%), **g** PEBAX 1074/PEG 400 (40 wt.%), **h** PEBAX 1657/PEG 400 (40 wt.%), **i**

PEBAX 2533/PEG 400 (40 wt.%), **j** PEBAX 1074/PEG 1000 (20 wt.%), **k** PEBAX 1657/PEG 1000 (20 wt.%), **l** PEBAX 2533/PEG 1000 (20 wt.%), **m** PEBAX 1074/PEG 1000 (40 wt.%), **n** PEBAX 1657/PEG 1000 (40 wt.%), and **o** PEBAX 2533/PEG 1000 (40 wt.%)

Table 3 Effects of PEG 400 loading on the permeabilities to gaseous CO₂ and CH₄ and the ideal CO₂/CH₄ selectivities of the prepared membranes at 2 bar and 25 °C

Prepared membrane	Permeability (barrer)		Ideal CO ₂ /CH ₄ selectivity
	CO ₂	CH ₄	
Neat PEBAX 1074	64.8	3.2	20.2
PEBAX 1074/PEG 400 10 wt.%	105.6	5.2	20.3
PEBAX 1074/PEG 400 20 wt.%	132.3	6.5	20.4
PEBAX 1074/PEG 400 30 wt.%	151.3	7.3	20.6
PEBAX 1074/PEG 400 40 wt.%	168.4	8.1	20.8
Neat PEBAX1657	72.2	3.9	18.5
PEBAX 1657/PEG 400 10 wt.%	114.6	6.2	18.6
PEBAX 1657/PEG 400 20 wt.%	141.9	7.5	18.9
PEBAX 1657/PEG 400 30 wt.%	156.9	8.2	19.1
PEBAX 1657/PEG 400 40 wt.%	174.5	9.1	19.2
Neat PEBAX 2533	191.0	26.6	7.2
PEBAX 2533/PEG 400 10 wt.%	247.7	34.1	7.2
PEBAX 2533/PEG 400 20 wt.%	282.6	38.5	7.3
PEBAX 2533/PEG 400 30 wt.%	302.2	40.6	7.4
PEBAX 2533/PEG 400 40 wt.%	319.4	42.2	7.6

incorporating a high molecular mass PEG causes nonuniform miscibility of the two polymers, leading to an irregular and convoluted blend membrane structure, as illustrated by Fig. 4j–o [7].

Permeation experiments

Effect of PEG incorporation

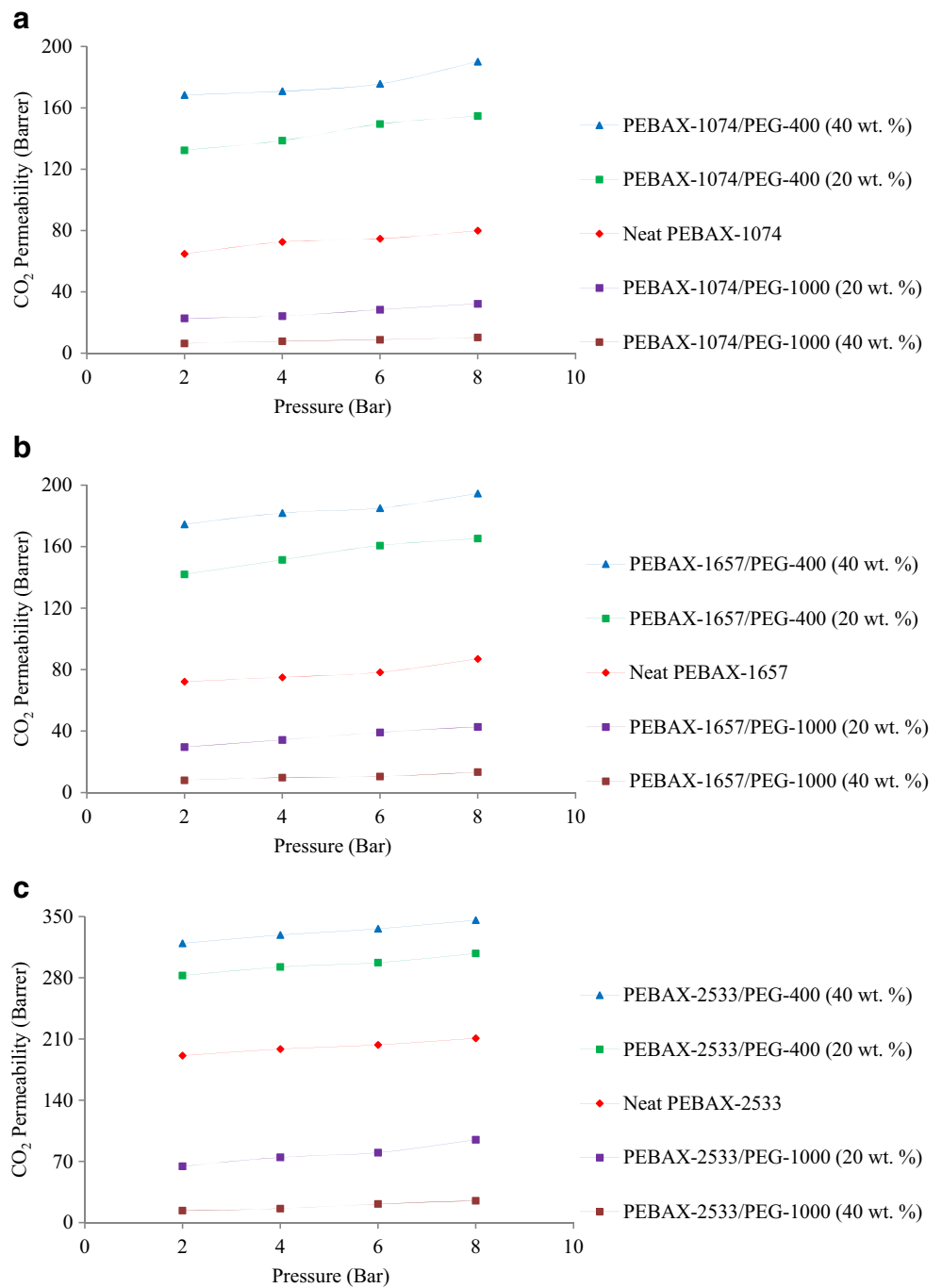
Tables 3 and 4 show the membrane permeabilities to pure gaseous CO₂ and CH₄ and the ideal CO₂/CH₄ selectivity as

functions of the PEG 400 or PEG 1000 loading. From the results presented, it is clear that increasing the PEG 400 content in the blend membrane enhances the permeation of pure gaseous CO₂ and CH₄ considerably while only slightly affecting the ideal CO₂/CH₄ selectivity. However, increasing the PEG 1000 content in the blend membranes significantly decreases the permeation of pure gaseous CO₂ and CH₄ and substantially increases the ideal CO₂/CH₄ selectivity. This behavior of the CO₂ and CH₄ gas permeabilities can be attributed to the influence of the molecular mass of the PEG on the microphase structure of the polymer blend.

Table 4 Effects of PEG 1000 loading on the permeabilities to gaseous CO₂ and CH₄ and the ideal CO₂/CH₄ selectivities of the prepared membranes at 2 bar and 25 °C

Prepared membrane	Permeability (barrer)		Ideal CO ₂ /CH ₄ selectivity
	CO ₂	CH ₄	
Neat PEBAX 1074	64.8	3.2	20.2
PEBAX 1074/PEG 1000 10 wt.%	47.9	2.1	22.7
PEBAX 1074/PEG 1000 20 wt.%	228	0.9	24.7
PEBAX 1074/PEG 1000 30 wt.%	9.8	0.4	25.9
PEBAX 1074/PEG 1000 40 wt.%	6.3	0.2	27.1
Neat PEBAX 1657	72.2	3.9	18.5
PEBAX 1657/PEG 1000 10 wt.%	51.0	2.4	21.1
PEBAX 1657/PEG 1000 20 wt.%	29.7	1.3	23.3
PEBAX 1657/PEG 1000 30 wt.%	15.2	0.61	24.5
PEBAX 1657/PEG 1000 40 wt.%	8.0	0.3	25.6
Neat PEBAX 2533	191.1	26.6	7.2
PEBAX 2533/PEG 1000 10 wt.%	107.6	12.8	8.4
PEBAX 2533/PEG 1000 20 wt.%	64.4	6.8	9.5
PEBAX 2533/PEG 1000 30 wt.%	43.4	4.2	10.2
PEBAX 2533/PEG 1000 40 wt.%	13.7	1.2	10.9

Fig. 5a–c Effects of the feed pressure on the CO₂ permeabilities of the membranes fabricated with different grades of PEBAXs and PEGs: **a** PEBAX 1074, **b** PEBAX 1657, **c** PEBAX 2533

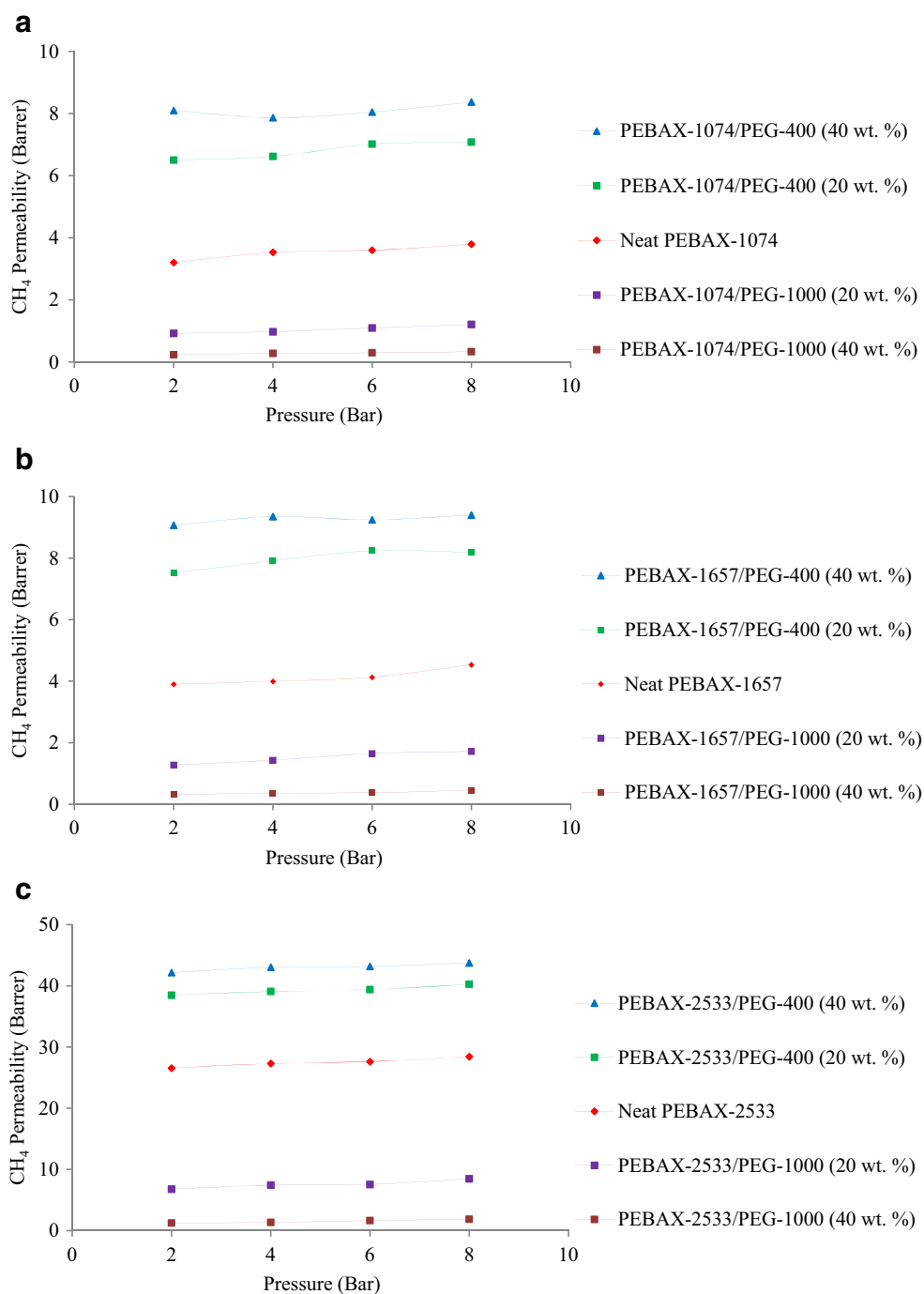


PEG 400, with its high chain mobility, is amorphous, and causes decrystallization of both types of segments when added to the PEBAX matrix, thus increasing the amorphous region for gas transport. In other words, adding PEG 400 increases the amount of amorphous EO segments and thus the free volume of the membrane. On the other hand, PEG 1000, with its low chain mobility, is crystalline, and causes crystallization of both types of segments when added to the PEBAX matrix, thus decreasing the amorphous region for gas transport. In other

words, adding PEG 1000 decreases the amount of amorphous EO segments and the free volume of the membrane [7, 20, 23, 26].

Also, PEG 400 shows good miscibility with the PEBAXs, whereas PEG 1000 shows poor miscibility with the PEBAXs and phase separation. The lower miscibility of PEG 1000 than that of PEG 400 can be attributed to differences in their chemical structures: PEG 400 has eight EO units for two hydroxyl end groups, while PEG 1000 has twenty EO units. The better miscibility of the lower molecular mass PEG is understandable

Fig. 6a–c Effects of the feed pressure on the CH_4 permeabilities of the membranes fabricated with different grades of PEBAXs and PEGs: **a** PEBAX 1074, **b** PEBAX 1657, **c** PEBAX 2533

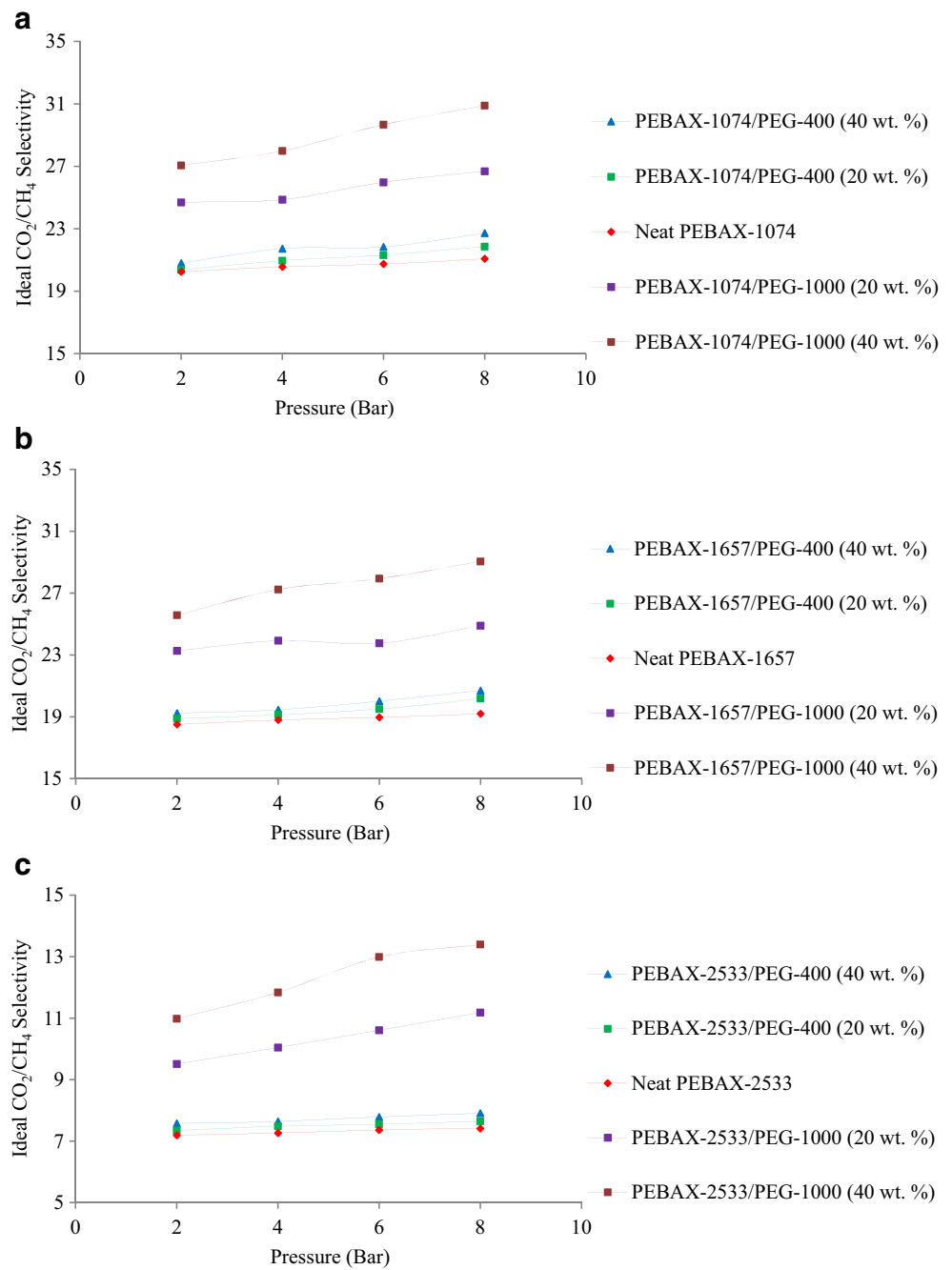


if the favorable mixing enthalpy caused by the hydrogen bonds between PEG hydroxyl end groups and ether groups in the PEBAXs is considered [7, 19, 39].

The incorporation of PEG 400 increases gas permeability, which can be attributed to the higher solubility caused by the presence of more ethylene oxide (EO) units, as well as the higher diffusivity due to the increased free volume (either the total fractional free volume or the individual free volume space): at higher PEG contents, there are more segmental motions since the lower molecular

mass PEG acts as a plasticizer between PEBAX chain segments to screen out polymer–polymer interactions and generate additional intermolecular space for small Brownian motion. However, the incorporation of PEG 1000 decreases the gas permeability. This can be ascribed to a tradeoff between the higher solubility caused by more EO units and the reduced diffusivity due to the smaller free volume at higher PEG contents. There would therefore be reduced motion in the PEBAX segments since a higher molecular mass PEG acts as a stiffener between PEBAX chain

Fig. 7a–c Effects of the feed pressure on the ideal CO₂/CH₄ selectivities of the membranes fabricated with different grades of PEBAXs and PEGs: **a** PEBAX 1074, **b** PEBAX 1657, **c** PEBAX 2533



segments to screen out polymer/polymer interactions and reduce additional intermolecular space for small Brownian motion [7, 19, 20, 26, 40].

As explained, the addition of the polar ether groups of PEG 400 enhances the affinity of CO₂ for the polymer matrix, increasing the membrane’s solubility selectivity. However, it also increases the chain spacing, which decreases the membrane’s molecular sieve properties as well as its diffusivity selectivity. Therefore, the total selectivity, which is the product of the diffusivity and solubility selectivities, increases slightly. However, the addition of the polar ether

groups of PEG 1000 enhances the affinity of CO₂ for the polymer matrix, increasing the membrane’s solubility selectivity. Furthermore, it decreases the chain spacing, which increases the membrane’s molecular sieving ability as well as its diffusivity selectivity. Thus, the total selectivity increases considerably in this case [7, 20, 26].

Effect of the feed pressure

Pressure affects the gas permeability through a membrane in several respects. First, increasing the pressure leads to a more

compact membrane matrix, which may in turn reduce the free volume and gas diffusion. Second, it is a driving force for gas transport through the membrane. Third, as the pressure is increased, it increases the gas concentration, enhancing the solubility of the gas in the membrane. Since the gas permeability coefficient is obtained by multiplying the diffusion and solubility coefficients, gas permeation increases when the solubility coefficient increases [26, 41].

The effects of increasing the feed pressure from 2 to 8 bar on the performance of the prepared membranes are illustrated in Figs. 5, 6, and 7. For all the blend membranes, as the pressure increases, the CO₂ and CH₄ permeabilities and the ideal CO₂/CH₄ selectivity continuously increase. Based on the definition of the permeability coefficient, the increases in the permeabilities of both gases are mainly due to the increased driving force. They may also be due to the enhanced gas concentration (solubility) [7, 32].

Furthermore, under the same conditions, the ideal CO₂/CH₄ selectivity increased with increasing feed pressure for all membranes prepared using the 1074, 1657, and 2533 grades of PEBAX. Compared to CH₄, CO₂ is a more condensable gas with considerable affinity for the PE segments of polymer chains, and it has a smaller kinetic diameter of 3.3 Å than CH₄ (3.8 Å), meaning that it shows higher permeabilities through the prepared membranes [7]. Additionally, CO₂ permeability can be increased by plasticization to a greater extent than CH₄ can, which is related to the nature of CO₂ gas [42].

The trend for increased permeation of the blend membranes incorporating PEG 400 with increased feed pressure was more noticeable for membranes with low PEG 400 contents. This indicates that, when the PEG 400 content is high, the relatively high number of amorphous segments leads to a greater loss of crystallinity. Consequently, more free volume is created, so greater gas diffusion is obtained. Therefore, the effect of membrane compactness becomes stronger as the PEG 400 content increases, meaning that the increase in gas permeation with feed pressure is less noticeable for membranes with high PEG 400 contents than for those with low PEG 400 contents. However, the increase

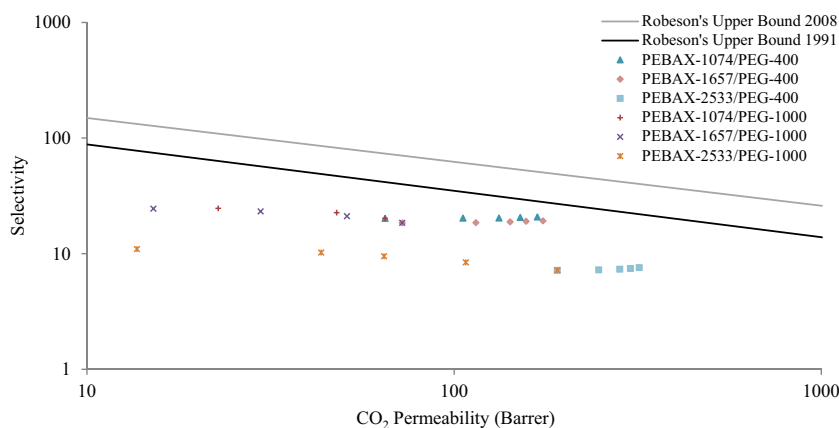
in permeation with feed pressure is more significant for blend membranes with high PEG 1000 contents than for those with low PEG 1000 contents. This illustrates that there is less loss of crystallinity in membranes with high PEG 1000 contents than in those with low PEG 1000 contents because there are fewer amorphous segments in the former. As a result, more free volume and greater gas diffusion are obtained. Accordingly, the effect of the driving force becomes more apparent for membranes with high PEG 1000 contents, meaning that gas permeation increases more markedly through those membranes [41].

Comparison with the Robeson diagram

A standard comparison of the gas separation properties of the different membranes was performed by examining selectivity vs. permeability plots (Robeson diagrams) for the membranes. The aim of most research in this field is to get as close as possible to the bound limit of such a diagram (called Robeson's upper bound [8, 43]). To compare the results of the current work with Robeson's upper bound, performance data were obtained for the prepared membranes at a standard temperature and pressure of 25 °C and 2 bar, respectively; see Fig. 8.

When compared with Robeson's upper bound, the membranes prepared with PEBAX 1074 as the base polymer presented the best separation performance, followed by the membranes prepared with PEBAX 1657, while the membranes prepared with PEBAX 2533 presented the worst separation performance. Also, the data for membranes with PEG 400 are closer to Robeson's upper bound than the data for the neat membranes are. Increasing the PEG 400 content in the membrane pushes the data closer to Robeson's upper bound. On the other hand, the data for the membranes with PEG 1000 are further from Robeson's upper bound than the data for the neat membranes, and increasing the PEG 1000 content increases the distance between the data and Robeson's upper bound.

Fig. 8 Comparison of the CO₂/CH₄ separation performance of each of the prepared membranes with the Robeson upper bound



Conclusion

In the present study, the CO₂/CH₄ separation performance was investigated for various membranes generated by blending low and high molecular mass PEGs with PEBAX polymers with different PE contents. These blend membranes were prepared by incorporating one of two types of PEG (with molecular masses of 400 and 1000 g mol⁻¹) with one of three grades of PEBAX with different PE contents (namely PEBAX 1074, PEBAX 1657, and PEBAX 2533). The PEGs, which were used as blending agents, were incorporated at mass fractions ranging from 10 to 40 wt.% based on the mass of the PEBAX. The gas separation performance characteristics of the neat and blend membranes, comprising their CO₂ and CH₄ permeabilities and their ideal CO₂/CH₄ selectivities, were studied at room temperature (25 °C) and in the pressure range 2–8 bar. The structural features of the prepared membranes were characterized using XRD analysis, with the results showing that increasing the filler content in the polymer matrix reduces the diffraction peaks of the crystalline region for different grades of PEBAX. This reduction in the crystallinity of the polymer can also occur due to the disruption of the interchain hydrogen bonds which connect the PA segments. ATR-FTIR analysis was also utilized to examine and compare the chemical bonds in the prepared membranes. The spectra of the membranes showed that as the PEG content in the prepared membranes is increased, some of the wavenumbers and intensities of some of the peaks characteristic of the neat PEBAX membranes change due to the rupture of interchain hydrogen bonds between the PA segments. Cross-sectional SEM images of all the blend membranes containing PEG 400 showed an irregular and convoluted membrane structure, whereas such images of membranes with PEG 1000 showed immiscibility and phase separation. The results of this work show that when a low molecular mass PEG is incorporated into a membrane, its permeability increases significantly but its ideal CO₂/CH₄ selectivity increases only slightly, whereas the incorporation of a high molecular mass PEG decreases membrane permeability considerably but also increases the ideal CO₂/CH₄ selectivity sharply. This behavior is particularly apparent for PEBAXs with low PE contents. Also, a comparison of the permeability/selectivity values of the prepared blend membranes with the upper bound in Robeson's diagram was carried out. The results obtained from this work highlight the potential applicability of the blend membranes to CO₂/CH₄ separation in natural gas sweetening processes, due to their improved separation properties.

Acknowledgments The authors would like to thank the Iran National Science Foundation (INSF) for supporting the research.

References

- Car A, Stropnik C, Yave W, Peinemann K-V (2008) Pebax[®]/polyethylene glycol blend thin film composite membranes for CO₂ separation: performance with mixed gases. *Sep Purif Technol* 62:110–117
- Rezaei M, Ismail AF, Hashemifard S, Bakeri G, Matsuura T (2014) Experimental study on the performance and long-term stability of PVDF/montmorillonite hollow fiber mixed matrix membranes for CO₂ separation process. *Int J Greenh Gas Control* 26:147–157
- Rahim NA, Ghasem N, Al-Marzouqi M (2015) Absorption of CO₂ from natural gas using different amino acid salt solutions and regeneration using hollow fiber membrane contactors. *J Nat Gas Sci Eng* 26:108–117
- Al-Rabiah AA, Ajbar AM, Soliman MA, Almalki FA, Abdelaziz OY (2015) Modeling of nitrogen separation from natural gas through nanoporous carbon membranes. *J Nat Gas Sci Eng* 26:1278–1284
- Cong H, Yu B, Tang J, Zhao XS (2012) Ionic liquid modified poly (2,6-dimethyl-1,4-phenylene oxide) for CO₂ separation. *J Polym Res* 19:9761
- Nie F, He G, Zhao W, Ju J, Liu Y, Dai Y (2014) Improving CO₂ separation performance of the polyethylene glycol (PEG)/polytrifluoropropylsiloxane (PTFPMS) blend composite membrane. *J Polym Res* 21:319
- Wang S, Liu Y, Huang S, Wu H, Li Y, Tian Z, Jiang Z (2014) Pebax-PEG-MWCNT hybrid membranes with enhanced CO₂ capture properties. *J Membr Sci* 460:62–70
- Robeson LM (2008) The upper bound revisited. *J Membr Sci* 320:390–400
- Chen Y, Wang B, Zhao L, Dutta P, Ho WW (2015) New Pebax[®]/zeolite Y composite membranes for CO₂ capture from flue gas. *J Membr Sci* 495:415–423
- Minhas FT, Farrukh S, Hussain A, Mujahid M (2015) Comparison of silica and novel functionalized silica-based cellulose acetate hybrid membranes in gas permeation study. *J Polym Res* 22:63
- Yave W, Car A, Peinemann K-V (2010) Nanostructured membrane material designed for carbon dioxide separation. *J Membr Sci* 350:124–129
- Azizi N, Mohammadi T, Behbahani RM (2017) Synthesis of a PEBAX-1074/ZnO nanocomposite membrane with improved CO₂ separation performance. *J Energy Chem* 26:454–465
- Bondar V, Freeman B, Pinnau I (2000) Gas transport properties of poly(ether-*b*-amide) segmented block copolymers. *J Polym Sci B Polym Phys* 38:2051–2062
- Rahman MM, Filiz V, Shishatskiy S, Abetz C, Neumann S, Bolmer S, Khan MM, Abetz V (2013) PEBAX[®] with PEG functionalized POSS as nanocomposite membranes for CO₂ separation. *J Membr Sci* 437:286–297
- Isanejad M, Azizi N, Mohammadi T (2016) Pebax membrane for CO₂/CH₄ separation: effects of various solvents on morphology and performance. *J Appl Polym Sci* 134(9). doi:10.1002/app.44531
- Rezakazemi M, Amooghin AE, Montazer-Rahmati MM, Ismail AF, Matsuura T (2014) State-of-the-art membrane based CO₂ separation using mixed matrix membranes (MMMs): an overview on current status and future directions. *Prog Polym Sci* 39:817–861
- Azizi N, Mohammadi T, Mosayebi Behbahani R (2017) Comparison of permeability performance of PEBAX-1074/TiO₂, PEBAX-1074/SiO₂ and PEBAX-1074/Al₂O₃ nanocomposite membranes for CO₂/CH₄ separation. *Eng Res Des* 117:177–189
- Li J, Wang S, Nagai K, Nakagawa T, Mau AWH (1998) Effect of polyethyleneglycol (PEG) on gas permeabilities and permselectivities in its cellulose acetate (CA) blend membranes. *J Membr Sci* 138:143–152

19. Yampolskii Y, Freeman B (eds)(2010) Membrane gas separation. Wiley, Chichester
20. Car A, Stropnik C, Yave W, Peinemann K-V (2008) PEG modified poly(amide-*b*-ethylene oxide) membranes for CO₂ separation. J Membr Sci 307:88–95
21. Azizi N, Mohammadi T, Behbahani RM (2017) Synthesis of a new nanocomposite membrane (PEBAX-1074/PEG-400/TiO₂) in order to separate CO₂ from CH₄. J Nat Gas Sci Eng 37:39–51
22. Zhao L, Chen Y, Wang B, Sun C, Chakraborty S, Ramasubramanian K, Dutta PK, Ho WW (2016) Multilayer polymer/zeolite Y composite membrane structure for CO₂ capture from flue gas. J Membr Sci 498:1–13
23. Mahmoudi A, Asghari M, Zargar V (2015) CO₂/CH₄ separation through a novel commercializable three-phase PEBA/PEG/NaX nanocomposite membrane. J Ind Eng Chem 23:238–242
24. Ghadimi A, Amirilargani M, Mohammadi T, Kasiri N, Sadatnia B (2014) Preparation of alloyed poly(ether *block* amide)/poly(ethylene glycol diacrylate) membranes for separation of CO₂/H₂ (syngas application). J Membr Sci 458:14–26
25. Ismail AF, Khulbe KC, Matsuura T (2015) Gas separation membrane materials and structures. Gas separation membranes: polymeric and inorganic. Springer International Publishing, Cham, pp. 37–192
26. Rabiee H, Ghadimi A, Abbasi S, Mohammadi T (2015) CO₂ separation performance of poly(ether-*b*-amide6)/PTMEG blended membranes: permeation and sorption properties. Chem Eng Res Des 98:96–106
27. Hosseinzadeh Beiragh H, Omidkhan M, Abedini R, Khosravi T, Pakseresht S (2016) Synthesis and characterization of poly(ether-*block*-amide) mixed matrix membranes incorporated by nanoporous ZSM-5 particles for CO₂/CH₄ separation. Asia-Pacific J Chem Eng 11:522–532
28. Stern SA (1968) The “barrer” permeability unit. J Polym Sci Polym Phys 6:1933–1934
29. Kim JH, Lee YM (2001) Gas permeation properties of poly(amide-*b*-ethylene oxide)–silica hybrid membranes. J Membr Sci 193: 209–225
30. Sridhar S, Suryamurali R, Smitha B, Aminabhavi TM (2007) Development of crosslinked poly(ether-*block*-amide) membrane for CO₂/CH₄ separation. Colloids Surf A 297:267–274
31. Surya Murali R, Ismail AF, Rahman MA, Sridhar S (2014) Mixed matrix membranes of Pebax-1657 loaded with 4A zeolite for gaseous separations. Sep Purif Technol 129:1–8
32. Zhao D, Ren J, Li H, Li X, Deng M (2014) Gas separation properties of poly(amide-6-*b*-ethylene oxide)/amino modified multi-walled carbon nanotubes mixed matrix membranes. J Membr Sci 467:41–47
33. Sridhar S, Smitha B, Suryamurali R, Aminabhavi TM (2008) Synthesis, characterization and gas permeability of an activated carbon-loaded PEBAX 2533 membrane. Des Monomers Polym 11:17–27
34. Dai Z, Bai L, Hval KN, Zhang X, Zhang S, Deng L (2016) Pebax[®]/TSIL blend thin film composite membranes for CO₂ separation. Sci China Chem 59:538–546
35. Ehsani A, Pakizeh M (2016) Synthesis, characterization and gas permeation study of ZIF-11/Pebax[®] 2533 mixed matrix membranes. J Taiwan Inst Chem Eng 66:414–423
36. Choi MC, Jung JY, Yeom HS, Chang YW (2013) Mechanical, thermal, barrier, and rheological properties of poly(ether-*block*-amide) elastomer/organoclay nanocomposite prepared by melt blending. Polym Eng Sci 53:982–991
37. Nafisi V, Hägg M-B (2014) Development of dual layer of ZIF-8/PEBAX-2533 mixed matrix membrane for CO₂ capture. J Membr Sci 459:244–255
38. Pavia DL, Lampman GM, Kriz GS (1979) Introduction to spectroscopy: a guide for students of organic chemistry. W.B. Saunders Co., Philadelphia
39. Gnanou Y, Fontanille M (2008) Organic and physical chemistry of polymers. Wiley, Hoboken
40. Yave W, Car A, Peinemann K-V, Shaikh MQ, Rätzke K, Faupel F (2009) Gas permeability and free volume in poly(amide-*b*-ethylene oxide)/polyethylene glycol blend membranes. J Membr Sci 339: 177–183
41. Rabiee H, Ghadimi A, Mohammadi T (2015) Gas transport properties of reverse-selective poly(ether-*b*-amide6)/[Emim][BF₄] gel membranes for CO₂/light gases separation. J Membr Sci 476: 286–302
42. Van Krevelen DW, Te Nijenhuis K (2009) Properties of polymers, 4th edn. Elsevier, Amsterdam
43. Robeson LM (1991) Correlation of separation factor versus permeability for polymeric membranes. J Membr Sci 62:165–185